

DOI: <http://dx.doi.org/10.21123/bsj.2021.18.1.0113>

DFT Calculations and Experimental Study to Inhibit Carbon Steel Corrosion in Saline Solution by Quinoline-2-One Derivative

Rehab Majed Kubba*

Mustafa Alaa Mohammed

Luma S. Ahamed

Department of Chemistry, College of Science, University of Baghdad, Baghdad, Iraq.

*Correspond author: Rehab_mmr_kb@yahoo.com, Mustafa.alaa602@yahoo.com, lumasami71@yahoo.com

*ORCID ID: <https://orcid.org/0000-0003-4855-7871>, <https://orcid.org/0000-0001-7575-3558>, <https://orcid.org/0000-0002-6482-6747>

Received 24/2/2020, Accepted 15/5/2020, Published Online First 6/12/2020, Published 1/3/2021



This work is licensed under a [Creative Commons Attribution 4.0 International License](https://creativecommons.org/licenses/by/4.0/).

Abstract:

A theoretical and protection study was conducted of the corrosion behavior of carbon steel surface with different concentrations of the derivative (Quinolin-2-one), namely (*1-Amino-4,7-dimethyl-6-nitro-1H-quinolin-2-one* (ADNQ2O)). Theoretically, Density Functional Theory (DFT) of B3LYP/ 6-311++G (2d, 2p) level was used to calculate the optimized geometry, physical properties and chemical inhibition parameters, with the local reactivity to predict both the reactive centers and to locate the possible sites of nucleophilic and electrophilic attacks, in vacuum, and in two solvents (DMSO and H₂O), all at the equilibrium geometry. Experimentally, the inhibition efficiencies (%IE) in the saline solution (of 3.5%) NaCl were studied using potentiometric polarization measurements. The results revealed that the (%IE) for carbon steel corrosion by ADNQ2O is (**89.88%**). The obtained thermodynamic parameters support the physical adsorption mechanism. The adsorption followed the Langmuir isotherm. The surface change on carbon steel was studied using SEM (Scanning Electron Microscopy).

Key words: Corrosion Behavior, DFT, Quinoline, Thermodynamic parameters.

Introduction

Corrosion inhibitor is a chemical substance that interacts with the surface or environment of a metal to which is exposed and acts to protect surface of the metal from corrosion (1). In general organic compounds with heterogeneous atoms (nitrogen, oxygen, and sulfur) in their aromatic composition are successfully used as corrosion inhibitors (2).

The high density of electrons on heterogeneous atoms in organic compounds is often has a tendency to resist corrosion. Quantitative chemical calculations were used to explain the mechanism of the corrosion reaction and to solve the chemical puzzle (3-6). This is a useful approach for investigating the mechanism of reaction of the inhibitor molecule on the metal surface. The geometry and electronic parameters of the inhibitor molecule can be obtained by theoretical calculations using computational methodologies for quantum chemistry. Quinoline derivatives are one of the important constituents of pharmacologically active synthetic compounds (7), including biological activities (8). Numerous reports have been presented in the literature for using quinoline and

some of its derivatives as corrosion inhibitors in various media (9-13). The aim of this search is focused on quinolin-2-one derivative (ADNQ2O), a heterocyclic entity and pharmacologically important molecule prepared by Al-Bayati RI. et. al. (14); experimentally, in salty (3.5% NaCl) solution using potentiostat method, and theoretically, the calculations of quantum chemical parameters were done in three media (vacuum, DMSO and water) using DFT of B3LYP/ 6-311++G (2d, 2p) level theory and Gaussian 09 program.

Materials and Methods:

Preparation of Carbon Steel

Carbon steel's rod symbolized as (C45) having the following percentage of metallic materials in composition (wt %): 0.122% C, 0.206% Si, 0.641% Mn, 0.016% P, 0.031% S, 0.118% Cr, 0.02% Mo, 0.105% Ni, and 0.451% Cu (3). The rod mechanically is cut into pieces forming a cyclic specimen of carbon steel a with 1.6 cm diameter and 3 mm thickness, each one of these specimen was refined with emery paper (silicon carbide SiC) in different grades (80, 150, 220, 320, 400, 1000, 1200

and 2000). Then washed with tap water, distilled water and acetone. Finally the specimen are held in a desiccators after dried in room temperature.

Preparation Solution

Blank Salt Solution

An amount of 35gm of sodium chloride (NaCl) was dissolved in (100 mL) distal water; the formative solution was transferred into (1L) volumetric flask, containing 2mL of dimethyl sulfoxide (DMSO). The volume of the solution was completed to (1L) by adding distilled water. Using (3.5%) NaCl is the suitable choice in this study in order to avoid some problems related to the ohmic drop.

Preparation the Salty Solutions of (ADNQ2O)

Three concentrations of the ADNQ2O inhibitor (5, 10, and 20)ppm were prepared by dissolving (0.005, 0.01 and 0.02)gm, respectively in (2mL) of DMSO, then transferred to (1L) volumetric flask containing 35gm (3.5%) of NaCl dissolved in distilled water. The volume of each solution was completed to 1L with distilled water.

Measurements of the Electronic Reactions

Potentiostatic Polarization

The potentiostat set up includes host computer, Mat lab, magnetic stirrer, thermostat, potentiostat, and galvanostat. The main part of the apparatus is the corrosion cell; it is made of Pyrex with 1000 mL capacity. This cell consists of two external and internal bowls. Three electrodes are mainly present in the electrochemical corrosion cell, carbon steel specimen having 1cm^2 surface area represented as a working electrode that is used to determine the working electrode potential due to another electrode namely reference electrode putting in a close to the working electrode. The reference

electrode is (Ag/AgCl, 3.0M KCl). The last electrode is a platinum auxiliary electrode having 10cm length. The starting step was represented by immersing working electrode in test solution for a period (of 15 minutes), to establish the potential of the open-circuit stable state (E_{ocp}). This possibility was observed to start electrochemical measurements in the range of ± 200 mV. All tests were done at (293, 303, 313 and 323) K.

Results and Discussion:

Theoretical Calculations

The nature of the geometrical structural of the organic inhibitors and their inhibition mechanism were described by (DFT) method. The inhibition efficiencies of compound (ADNQ2O) was investigated by theoretical corrosion inhibition parameters such as energy of E_{HOMO} (energy of the highest occupied molecular orbital) and E_{LUMO} (energy of the lowest unoccupied molecular orbital), E_{gap} (energy gap between E_{HOMO} and E_{LUMO}), μ (dipole moment), χ (electronegativity), EA (electron affinity), η (global hardness), S (softness), IE (ionization energy), ω (global electrophilicity), ΔN (the fraction of electrons transferred) and E_{tot} (the total energy) (15).

Optimized Molecular Geometry

The organic inhibitors compound was built in two dimensions structure by using Chem-Draw of Mopac program, (Fig. 1a). Gaussian 09 packages (16) were carried out for calculating the fully optimized structure in vacuum, using quantum mechanical method of DFT of Becke's three-parameter of Lee, Yang and Parr (B3LYP) with 6-311++G/(2d, 2p) level of theory (17-19) (Fig. 1b). In addition to vacuum, the equilibrium geometry was calculated in two solvents (DMSO and H_2O).

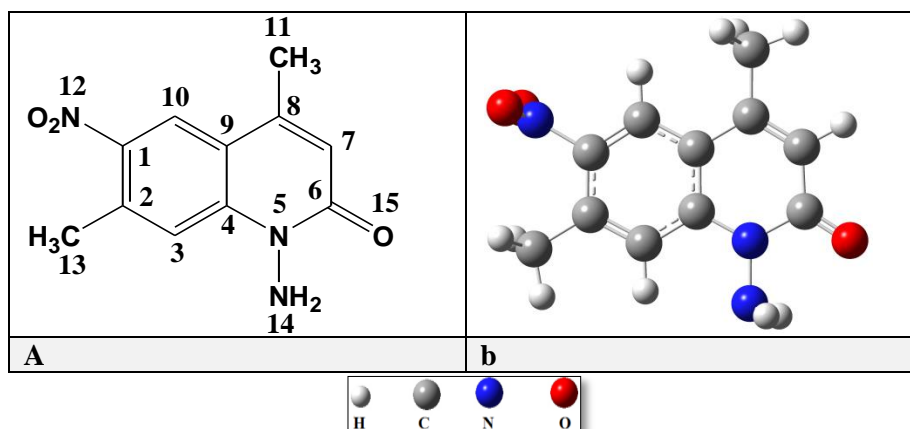


Figure 1. a. Two dimensions structure of (1-amino-4,7-dimethyl-6-nitro-1H-quinolin-2-one (ADNQ2O)) with the numbering of atoms, b. Three dimensions optimized structure of ADNQ2O calculated by DFT method.

Table (1) displays the geometrical structure details of ADNQ2O compound such as bond lengths, bond angles and dihedral angles which were calculated in three media (vacuum, (DMSO, and H₂O) using DFT method. The optimized geometrical structure is the same in the three media. Table (1) shows that in ADNQ2O compound, the C2-C13

owns the longest bond length of 1.502(Å), and the N14-H bond is the shortest bond with 1.011(Å) length. The values of the dihedral angles (cis & trans) indicate the planarity of the compound within (C_s) point group (cis dihedral angles are 0.00 and trans dihedral angles are 180.00 degree) (15).

Table 1. Geometrical structure for ADNQ2O inhibitor in three media (vacuum, DMSO and H₂O) as calculated using DFT method.

Bond	Bond length (Å)	Angle	Angle (degree)	Dihedral angle	Dihedral angle (degree)
C1-C2	1.398	C2C1C10	122.809	C10C1C2C3	0.0
C1-C10	1.374	C2C1N12	119.354	C10C1C2C13	180.0
C1-N12	1.470	C1C2C3	117.012	C1C2C3C4	0.0
C2-C3	1.385	C1C2C13	121.503	C13C2C3C4	180.0
C2-C13	1.502	C2C3C4	121.613	C2C3C4C9	0.0
C3-C4	1.401	C2C3H	119.377	C2C3C4N5	180.0
C3-H	1.077	C3C4C9	120.293	C3C4N5N14	0.0
C4-C9	1.410	C3C4N5	120.918	C3C4N5C6	180.0
C4-N5	1.390	C4N5C6	123.922	C4N5C6C7	0.0
N5-C6	1.413	C4N5N14	118.004	C4N5C6O14	180.0
N5-N14	1.411	N5C6C7	115.074	N5C6C7C8	0.0
C6-C7	1.448	C7C6O15	125.024	N5C6C7H	180.0
C6-O15	1.222	C6C7C8	123.449	C6C7C8C9	0.0
C7-C8	1.353	C6C7H	114.963	C6C7C8C11	180.0
C8-C9	1.451	C7C8C11	120.551	C7C8C9C4	0.0
C8-C11	1.501	C8C9C10	122.467	C7C8C9C10	180.0
N12-O	1.232	C1N12O	117.376	C8C9C10H	0.0
N14-H	1.011	N5N14H	106.163	C8C9C10C1	180.0

Figures 2a shows the density distributions of *HOMO* and *LUMO* for the optimized geometry of EMNQ2O inhibitor (in vacuum). It was shown that both *HOMO* and *LUMO* are located at the plane of EMNQ2O molecule. This indicates that the preferred

active-sites for electrophilic and nucleophilic attacks are located and distributed within the planarity region around the phenyl, nitrogen and oxygen atoms (Fig. 2b) (15).

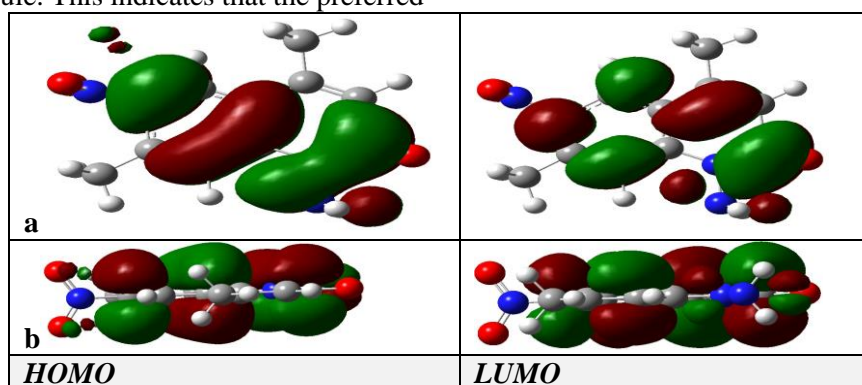


Figure 2. a- Density distributions of Frontier molecular orbitals of ADNQ2O compound, b- Planarity of ADNQ2O molecule. [Red color: negatively charged lobe; blue color: positive charge lobe]. Global Molecular Reactivity

Tables 2a and b show that ADNQ2O compound is a good inhibitor based on its values of the quantum corrosion efficiency parameters in the three media (vacuum and two polarity solvent). The high energy for *HOMO* corresponds to the more reactive molecule in the reactions with electrophiles, while low energy of *LUMO* is

essential for molecular reactions with nucleophiles. A high value of E_{HOMO} leads to increase inhibition efficiency of inhibitor molecule and vice versa for E_{LUMO} . μ (Dipole moment) is an important electronic parameter results from non-uniform distribution charges on the various atoms of molecule. High value of dipole moment increases the adsorption

between the inhibitor compound and the surface of the metal. IP (ionization potential), can be approximated by the negative energy of $HOMO$. Low values of IE increase the effectiveness of the inhibitor (20). EA is the amount of energy released when adding an electron to atom or molecule. High value of EA means less stable inhibitor (good corrosion inhibitor). η (chemical hardness) is a measure of the ability of atom or molecule to transfer the charge. Increasing η decreases the stability of molecule, so the inhibitor possessed low value of η is considered to be good inhibitor. S (chemical softness) is a measure of the flexibility of atom to receive electrons. Molecules having a high value of (S) are considered to be a good inhibitor (10). The electronegativity (χ) is the ability of atom or group to pull electrons; low electronegativity indicates a good inhibitor. (global electrophilicity index) is the measure of stability of atom after gaining electron. High value of (ω) meaning the molecule has a good inhibition. ΔN (difference in the number of electrons transferred). The fraction of electrons transferred (ΔN) from an inhibitor to carbon steel surface of ADNQ2O has

larger values in solvents compared with the vacuum, by the ability of ADNQ2O molecule to receive the electrons from the metallic surface by Fe atoms in the unoccupied orbital of ($3d$). This ability increases the inhibition efficiency (IE) when two systems, Fe and inhibitor, are brought together. The net results of the order for inhibition efficiency is $IE (H_2O) > IE (DMSO) > IE (vacuum)$, meaning IE increase with increasing the polarity of the medium. From this, we conclude that the stability of the inhibitor is higher in both solvents than in vacuum. Equations (1-8) were used for calculating the corrosion efficiency parameters (21-25):

$$IP = -E_{HOMO} \quad (1)$$

$$EA = -E_{LUMO} \quad (2)$$

$$\Delta E = E_{LUMO} - E_{HOMO} \quad (3)$$

$$\eta = (IP - EA) / 2 \quad (4)$$

$$\chi = (IP + EA) / 2 \quad (5)$$

$$S = 1 / \eta \quad (6)$$

$$\omega = (-\chi)^2 / 2\eta \quad (7)$$

$$\Delta N = (\chi_{Fe} - \chi_{inhib}) / [2(\eta_{Fe} + \eta_{inhib})] \quad (8)$$

Whereas χ_{Fe} is (7.00 eV mol^{-1}); η_{Fe} is $0.00 \text{ (eV mol}^{-1})$ for carbon steel.

Table 2.

a- Some physical properties of ADNQ2O inhibitor calculated by DFT at the optimized structure.

Inhibition medium	Point group	Molecular formula	E_{HOMO} (eV)	E_{LUMO} (eV)	$\Delta E_{LUMO-HOMO}$ (eV)	μ (Debye)	E_{total} (eV)
Vacuum	C_s	$C_{11}H_{11}N_3O_3$	-6.6482	-2.6673	3.981	1.1090	-22183.299
DMSO	C_s		-6.5923	-2.9065	3.686	0.8582	-22202.041
Water	C_s		-6.5921	-2.9095	3.683	0.8516	-22202.044

b- Quantum chemical parameters for ADNQ2O inhibitor calculated by DFT at the optimized structure.

Inhibition medium	IP (eV)	EA (eV)	η (eV)	χ (eV)	S (eV)	ω (eV)	ΔN
Vacuum	6.6482	2.6673	1.9905	4.6575	0.5023	5.4489	0.5884
DMSO	6.5923	2.9065	1.8430	4.7490	0.5425	6.1185	0.6106
Water	6.5921	2.9095	1.8415	4.7505	0.5430	6.1274	0.6107

Active Sites of ADNQ2O Inhibitor

The inhibition of ADNQ2O inhibitor was done by using DFT Mullikan's charge population analysis in (ecu), which gave indication of reactive centers of molecules (electrophilic and nucleophilic sites). For that, region that has a large electronic charge is chemically softer than the region that has a small electronic charge. Thus, the density of electron plays an important role in the chemical reactivity calculating. The chemical adsorption interactions are either by orbital interactions or electrostatic. The sites of nucleophilic attack is the place where the positive charge value is maximum, in turn, the site

of electrophilic attack is controlled by the negative charge value. The nucleophilic and electrophilic electronic charge values of ADNQ2O compound are higher in DMSO and H_2O solutions than in vacuum noting the increase in the stability of the compound by increasing the polarity of the solvent and leading to a decrease in the total energy of the compound, Table 2a. Table 3 shows that the order of the nucleophilic reactive sites of ADNQ2O inhibitor is as follows: $C1 > C4 > C3 > C7 > C10 > C11 > C15$; whereas the order of the electrophilic reactive sites is: $C2 > C9 > C8 > C6$.

Table 3. DFT Mulliken charge population analysis in ADNQ2O molecule calculated in three media (vacuum, DMSO, and H2O).

Atom	Electronic Charge (ecu)	Atom	Electronic charge (ecu)	Atom	Electronic Charge (ecu)	Atom	Electronic Charge (ecu)
C1	-1.171V	N5	-0.103V	C9	0.997V	C13	-0.095V
	-1.179D		-0.056D		1.003D		-0.097D
	-1.180H		-0.056H		1.003H		-0.097H
C2	1.339V	C6	0.307V	C10	-0.387V	N14	-0.170V
	1.306D		0.384D		-0.395D		-0.214D
	1.306H		0.386H		-0.395H		-0.214H
C3	-0.621V	C7	-0.508V	C11	-0.360V	O15	-0.491V
	-0.629D		-0.528D		-0.373D		-0.579D
	-0.630H		-0.528H		-0.374H		-0.580H
C4	-0.926V	C8	0.831V	N12	0.017V	-----	-----
	-0.895D		0.806D		0.079D		
	-0.894H		0.806H		0.080H		

V: vacuum phase; D: dimethyl sulfoxide; H: water; ecu: electron control unit.

Measurement of Corrosion Inhibition

Potentiodynamic Polarization Measurements

The parameters of the electrochemical corrosion are listed in Table 4 such as corrosion potential (E_{corr}), Tafel slopes (b_c and/or b_a) and corrosion current density (i_{corr}) obtained by cathodic and anodic regions of Tafel lines. IE%, Rp, θ , and CR can be measured using equations (8-11).

$$\%IE = \frac{i_{corr(un)} - i_{corr(in)}}{i_{corr(un)}} \times 100 \dots (8)$$

Whereas $i_{corr(in)}$ is the inhibited corrosion current densities, $i_{corr(un)}$ is the uninhibited current densities. The values of polarization

$$Rp = \frac{b_a \times b_c}{2.303(b_a + b_c) \times i_{corr}} \quad (9)$$

The surface coverage (θ) of carbon steel corrosion immersed in 3.5% NaCl containing different EMNQ2O concentrations (C) can be estimated using equation 10.

$$\theta = \frac{\%IE}{100} \quad (10)$$

The corrosion rate (CR) can be calculated by equation 11:

$$CR = i_{corr} \times 0.249 \dots (11)$$

The addition of quinolin-2-one derivative leads to decrease in the (CR) i.e the conversion of cathodic and anodic curves to lower values of the current density. Both cathode and anode corrosion reactions in C.S (carbon 45) electrode were prevented by ADNQ2O in 3.5% NaCl solution.

Figure 3 shows Tafel lines of anodic and cathodic polarization curves for the corrosion of carbon steel in salty solution, with and without the addition of various concentrations of ADNQ2O inhibitor as well as the optimum conditions of (20ppm) inhibitor and (at 293K) temperature. Table 4 lists (CR) values of C.S and inhibition efficiencies of various inhibitor concentrations measured at salty solution at different temperature. The table shows that increasing temperature lead to increase the corrosion current densities I_{corr} . While the efficiencies IE% is increased with the increasing of the inhibitor concentration. The optimum conditions for ADNQ2O in the salty solution were found at 293K temperature and 20ppm inhibition concentration both corresponded to the lowest I_{corr} of 37.84 ($\mu A.cm^{-2}$) and the maximum IE% of 94.98 (%). The values of iron corrosion rate CR are decreased with the increase of ADNQ2O concentration. The addition of the inhibitor to the blank solution increases the cathodic and anodic current densities without shifting the corrosion potential. The ADNQ2O inhibitor therefore can be described as a mixed-type inhibitor in which its inhibition action is caused by the adsorption process. The inhibition action is a proportional of the reduction reaction area on carbon steel surface (15).

Table 4. Electrochemical data of C.S corrosion in salty solution at different concentrations of ADNQ2O compound.

Inhibitor ppm	T (K)	E _{corr} (mV)	i _{corr} (μA.cm ⁻²)	bc (mV.dec ⁻¹)	ba (mV.dec ⁻¹)	IE%	Θ	CR
Blank	293	-408.0	133.13	-230.4	138.5	-----	-----	33.15
	303	-446.7	172.04	-279.6	110.2	-----	-----	42.84
	313	-491.2	189.34	-269.0	96.5	-----	-----	47.15
	323	-547.7	192.99	-252.9	84.4	-----	-----	48.05
5	293	-367.6	24.08	-83.0	53.2	81.91	0.819	6.00
	303	-438.5	28.42	-78.2	47.6	83.48	0.835	7.08
	313	-467.6	34.21	-83.3	63.1	81.93	0.819	8.52
	323	-499.4	39.84	-131.5	57.1	79.35	0.794	9.92
10	293	-345.0	18.30	-107.6	60.1	86.25	0.863	4.56
	303	-399.8	32.21	-100.3	57.0	81.27	0.813	8.02
	313	-455.7	40.10	-125.8	62.6	78.82	0.788	9.98
	323	-511.0	42.48	-116.4	78.2	77.98	0.780	10.58
20	293	-361.8	13.47	-48.0	39.4	89.88	0.899	3.35
	303	-422.2	24.0	-59.1	50.7	86.04	0.860	5.98
	313	-478.9	33.46	-69.1	46.5	82.32	0.823	8.33
	323	-495.5	43.40	-115.4	54.1	77.51	0.775	10.81

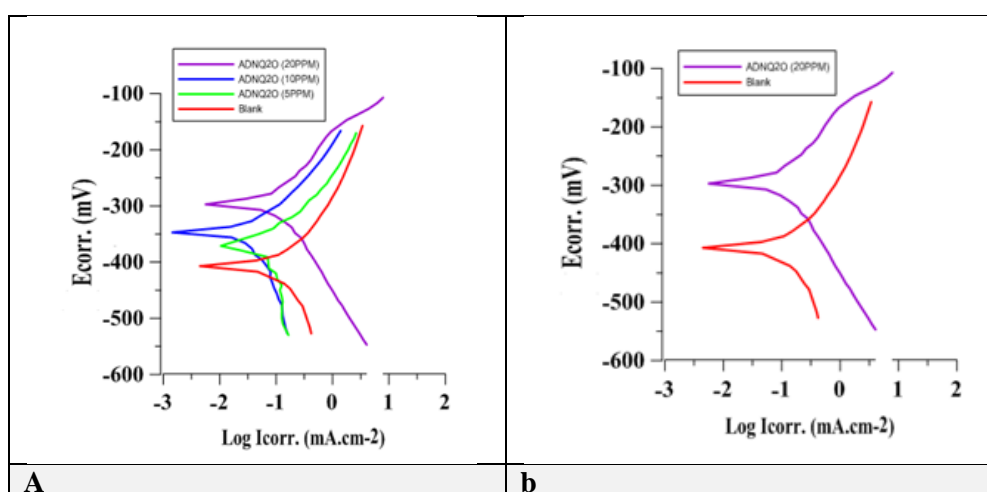


Figure 3. Polarization curve of carbon steel in salty solution at 293 (K) for ADNQ2O compound; (a) at different concentrations, and (b) at the optimum concentration.

Corrosion Kinetic and Thermodynamic Activation Parameters

Arrhenius law is presented as a straight line of the logarithm of the (CR). The activation parameters were calculated with and without inhibitor at different concentrations. The activation energy (E_a) of the corrosion process, and the pre-exponential factor (A), were calculating from equation 12, Fig. 4. All E_a values in presence of ADNQ2O inhibitor are higher than absence of it (blank) which is 09.6348 (kJ/ mol) for (3.5%) NaCl solution meaning that the corrosion reaction of C.S is retarded by ADNQ2O inhibitor. Plotting of log (CR/T) or log (I_{corr}/T) versus (1/T), gives a linear relationship with a slope of (-ΔH*/ 2.303R) and intercept of [log(R/ Nh)+ (ΔS*/ (2.303R))] equation (13), as shown in Fig. 5.

$$\text{Log } (I_{\text{corr}}) = \text{Log } A - E_a / (2.303RT) \quad (12)$$

$$\text{Log } (I_{\text{corr}}/ T) = \text{log } (CR/ T) = \text{Log } (R/ (N h)) + \Delta S^* / (2.303R) - \Delta H^* / (2.303RT) \quad (13)$$

Where (I_{corr}) is the corrosion current density which is equal to the corrosion rate (CR), (R) is the universal gas constant (8.314 J mol⁻¹ K⁻¹), (T) is the absolute temperature in K, (h) is Planck's constant (6.626 x 10⁻³⁴ J s), (N) is Avogadro's number (6.022 x 10²³ mol⁻¹), ΔH* is the enthalpy of activation and (ΔS*) is the entropy of activation.

Table 5 lists the activation thermodynamic parameters (ΔH* and ΔS*) which were calculated in salty solution. The positive values of (ΔH*) for the corrosion reaction in 3.5% NaCl solution at the temperature range of (293-323) K and different concentration support the endothermic nature of this reaction (16). Whereas negative values of (ΔS*) for the corrosion reaction indicate a decrease in the degree of freedom and consequently the inhibition action (17). ΔG* values for corrosion reaction were

calculated from equation 14. The positive values of ΔG^* indicating that the transition state of the adsorption process is not spontaneous.

$$\Delta G^* = \Delta H^* - T\Delta S^* \quad (14)$$

Table 5. Corrosion kinetic parameters for carbon steel in 3.5% NaCl in absence (blank) and presence various concentrations of ADNQ2O inhibitor.

Conc. (ppm)	ΔG^* (kJ/ mol)				ΔH^* (kJ/ mol)	ΔS^* (kJ/ mol K)	E_a^* (kJ/ mol)	A (Molecule/ cm ² S)
	293K	303K	313K	323K				
0 (Blank)	62.189	63.574	64.959	66.344	21.617	-0.1385	9.6348	1.10E+27
5	67.371	69.302	71.233	73.164	10.788	-0.1931	13.3442	8.59E+26
10	67.730	69.383	71.036	72.689	19.296	-0.1653	21.8526	2.44E+28
20	68.597	69.989	71.380	72.772	27.825	-0.1392	30.3808	5.65E+29

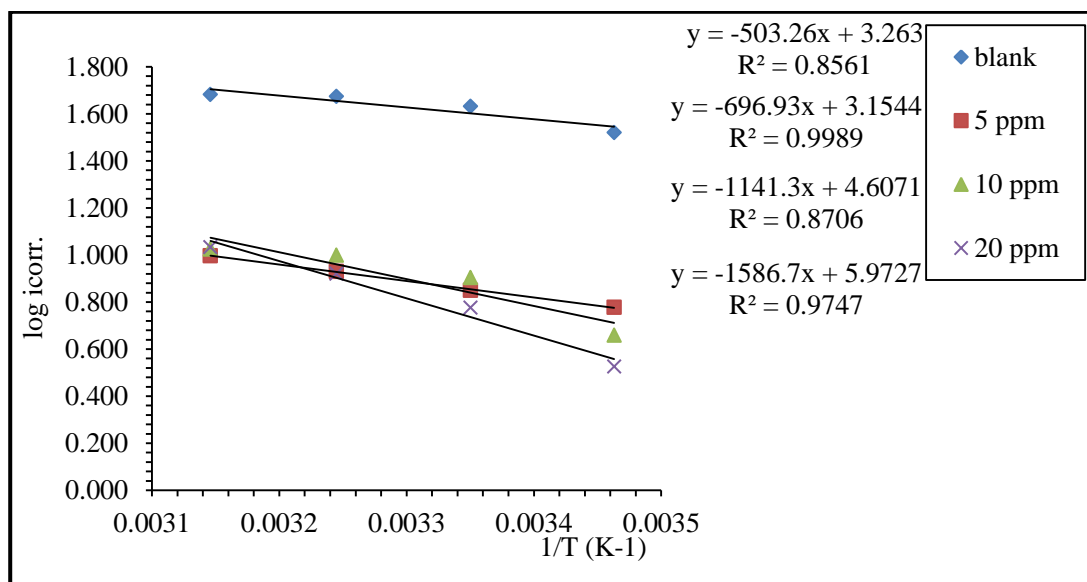
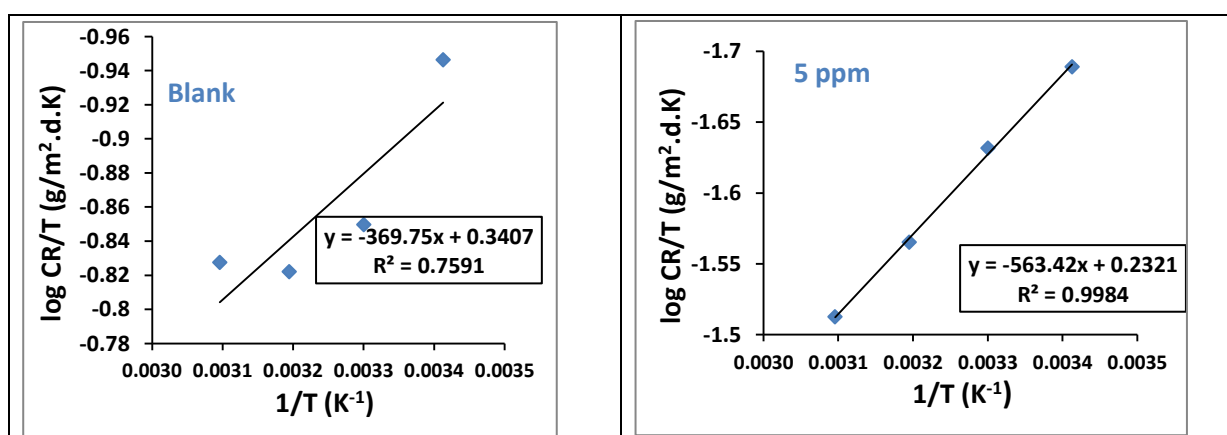


Figure 4. Plotting $\log (i_{corr})$ against $(1/T)$ for carbon steel in salty solution in absence (blank) and in presence of different concentrations of ADNQ2O inhibitor.



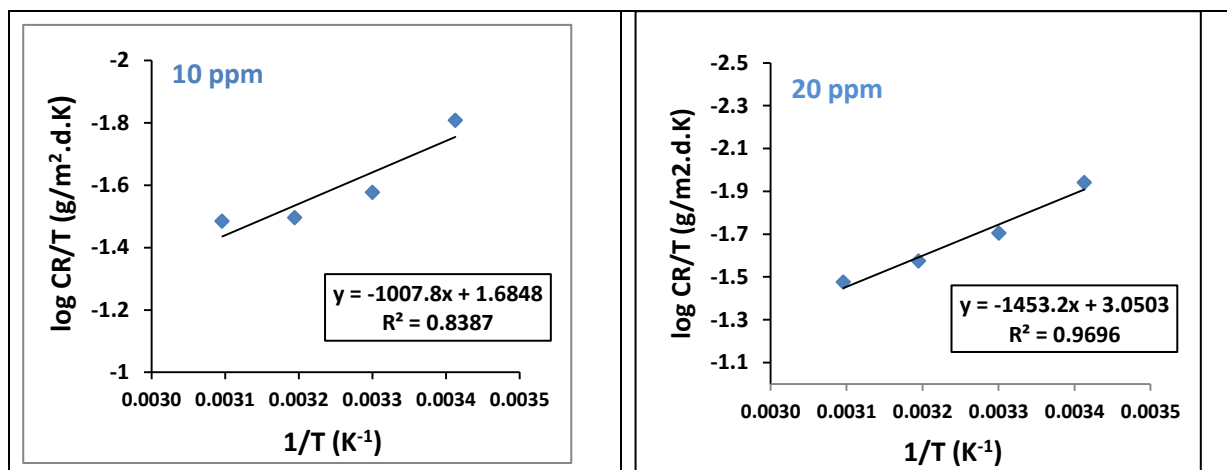


Figure 5. Plotting log (CR/T) against (1/T) of carbon steel in salty solution in absence (blank) and in presence of different concentrations of ADNQ2O inhibitor.

Adsorption of the Isotherms Process

The adsorption isotherms are essential in characterizing the reaction between carbon steel surface and inhibitor molecules. Langmuir adsorption isotherm is the most frequently used isotherms. It can be described by the following equation:

$$C/\theta = (1/K_{ads}) + C \quad (15)$$

Whereas C is the inhibitor concentration in 3.5% NaCl, K_{ads} is the adsorption equilibrium constant and θ is the surface coverage. The dependence of the (C/ θ) fraction as a function of (C) for ADNQ2O in salty solution is shown in Fig. 6. It can be used to determine K_{ads} . The adsorption equilibrium constant has a relation with the free energy of adsorption (ΔG_{ads}) through the following equation (15):

$$\Delta G_{ads} = -2.303 RT \text{Log}(55.55K_{ads}) \quad (16)$$

R is the gas constant ($J K^{-1} mol^{-1}$), T is the absolute temperature (K) and 55.5 is the molar concentration of water in the solution ($mol L^{-1}$). By rearranging the equation 16, plotting K_{ads} against (1/T), the ΔG_{ads} can be obtained from the slope (Fig. 7). Entropy values of adsorption (ΔS_{ads}°) and enthalpy values of adsorption (ΔH_{ads}°) were obtained by using equations (17 and 18).

$$\Delta G_{ads}^{\circ} = -RT \ln K_{ads} \quad (17)$$

$$\Delta G_{ads}^{\circ} = \Delta H_{ads}^{\circ} - T\Delta S_{ads}^{\circ} \quad (18)$$

Table 6 lists the thermodynamic functions of ADNQ2O inhibitor on C.S surface in 3.5% NaCl at various temperatures. Higher values of K_{ads} which is obtained from Langmuir isotherm for ADNQ2O indicate strong adsorption on the carbon steel in 3.5% NaCl. Negative values of ΔG_{ads}° indicate spontaneous adsorption process. The values of ΔG_{ads}° around -20 (kJ/mol) or less negative consisted with the electrostatic interaction (physisorption); while those values of -40 (kJ/mol) or more negative involve electron transfer which leads to form a chemical bond (chemisorptions) (26).

The values of ΔG_{ads}° were found in the range of -49.652 to -40.929 ($kJ mol^{-1}$) at different temperatures (293-323K). These values indicate that the adsorption of ADNQ2O follows physisorption processing. Positive value of the obtained entropy (ΔS_{ads}°) is confirming that the corrosion process is entropically favorable (19). The negative value of ΔH_{ads}° indicates an exothermic process for the adsorption of inhibitory ADNQ2O molecules on the C.S surface. For ADNQ2O, ΔH_{ads}° is equal to -89.442 ($kJ mol^{-1}$) (see table 6). ΔH_{ads}° can be also obtained from the integrated version of the Vant Hoff equation which is expressed by: $\ln K_{ads} = -\Delta H_{ads}^{\circ}/RT + \text{constant}$ (19)

Table 6. Thermodynamic parameters for adsorption of ADNQ2O compound on C.S surface in 3.5% NaCl at various temperatures.

T (K)	K_{ads} ($L mol^{-1} * 10^6$)	ΔG_{ads}° ($kJ. mol^{-1}$)	ΔH_{ads}° ($kJ.mol^{-1}$)	ΔS_{ads}° ($kJ.mol^{-1}$)	R^2
293	$3.008203 * 10^5$	-10.585	-36.666	0.263	1.0000
303	$4.571266 * 10^5$	-11.622			0.9987
313	$7.78717.9 * 10^5$	-12.942			0.9990
323	$11.91753 * 10^5$	-13.997			1.0000

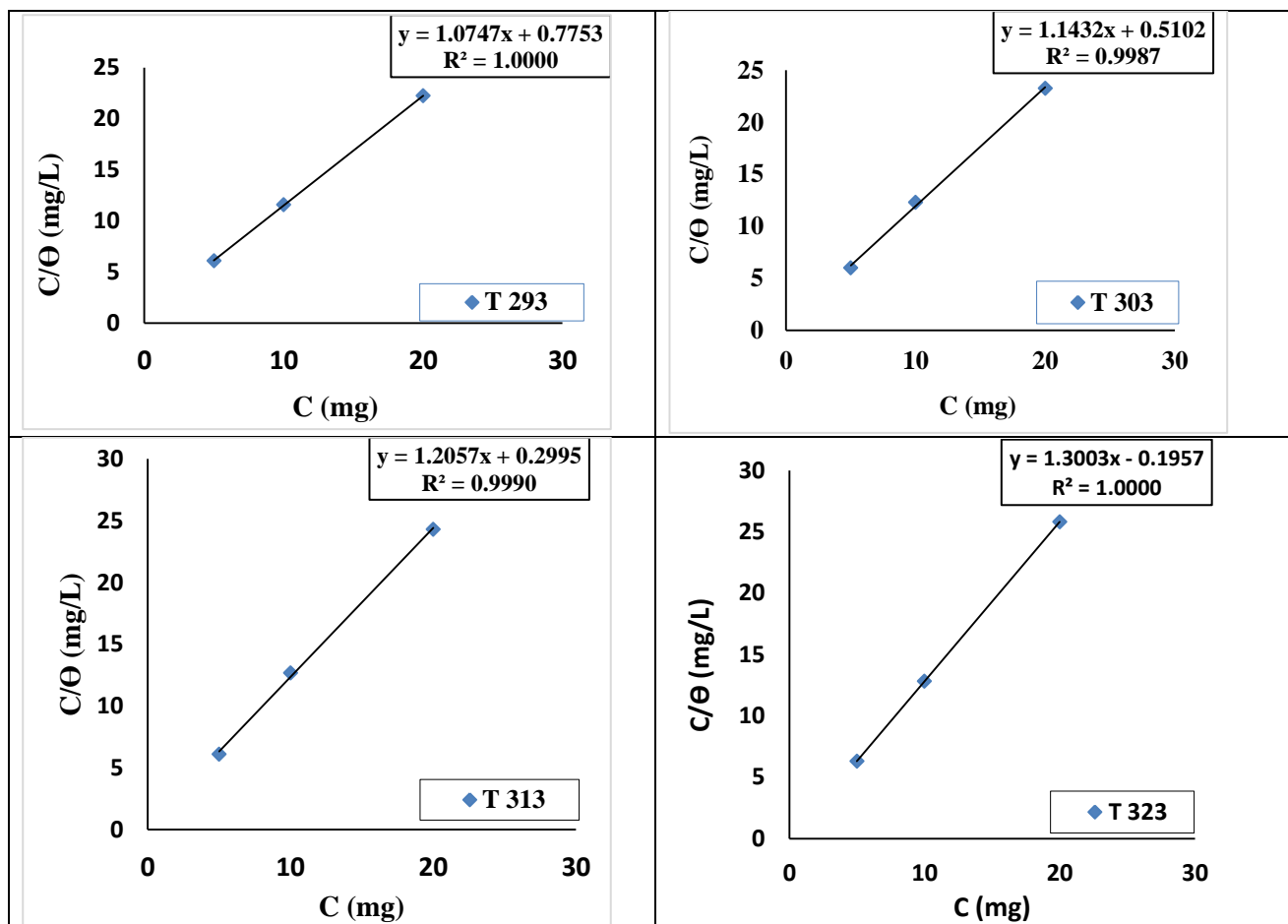


Figure 6. Langmuir isotherms plot for the adsorption ADNQ20 inhibitor on carbon steel in salty medium at temperatures of (293, 303, 313 and 323) K.

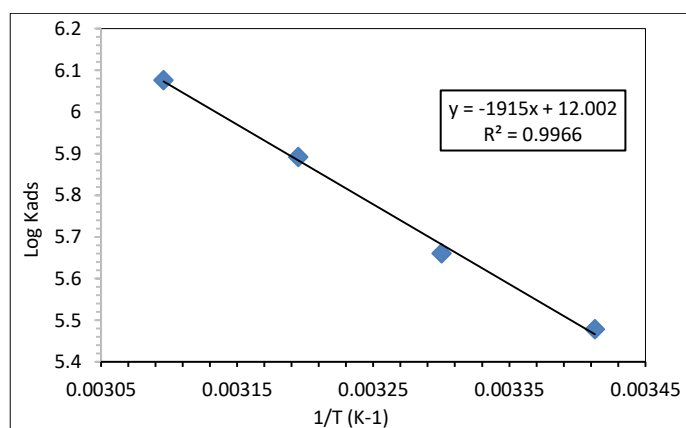


Figure 7. Plotting of $\log K_{ads}$ against $(1/T)$ for ADNQ20 compound.

Scanning Electron Microscopy (SEM):

SEM micrographs of the corroded carbon steel in 3.5% NaCl solution in the presence and absence of ADNQ20 inhibitor are shown in Fig. 8. In images (Fig. 8a) of this figure (absence of inhibitor), a clear damage is obvious on the metal

surface. In contrast, Fig. 8b shows a remarkable improvement in the metal surface morphology due to the presence of ADNQ20 inhibitor which is responsible for forming a protective film of an insoluble complex on carbon steel surface (Fe^{2+} -ADNQ20 complex) (27-28).

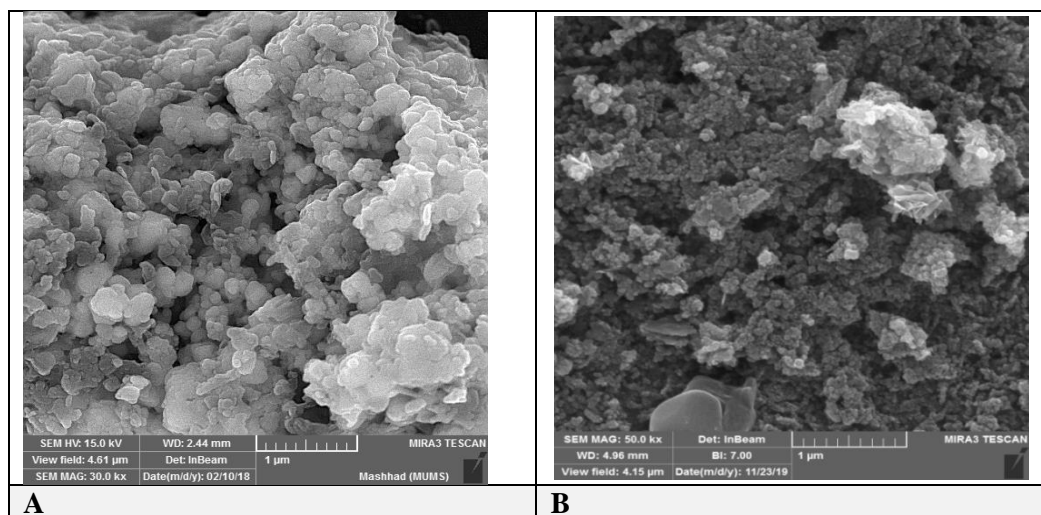


Figure 8. SEM image of C.S surface; (a) in salty medium of 3.5% NaCl solution in absence (blank) of ADNQ2O inhibitor, (b) in presence of 20 ppm of ADNQ2O inhibitor.

Conclusions:

- The values of the theoretical chemical parameters suggest that ADNQ2O has a great tendency to interact with the metal surface in solvent solutions than in vacuum, and it is a good inhibitor in both of them.
- The results of DFT calculations on ADNQ2O of quinoline derivative have been presented in vacuum, DMSO and in water solutions. The *HOMO*, *LUMO*, and charges on atoms predict a similar center that would prefer to be attacked by nucleophilic or electrophilic species.
- Theoretical calculations of (DFT/ B3LYP/ 6-311++G/ 2d, 2p) gave realistic results in the case of the geometry of the conformers, and the results of DFT/B3LYP were closer to the experimental data.
- Experimentally, it was observed that corrosion rates of carbon steel in the corrosive medium decreased with the addition of different concentrations of ADNQ2O inhibitor.
- ADNQ2O inhibition efficiency in the salt solution was (89.88%). However the thermodynamic and kinetic parameters suggest that ADNQ2O has greater tendency to interact with the metal surface in (3.5%) NaCl solution and it is a very good inhibitor for protection carbon steel surface in salty solution.

Authors' declaration:

- Conflicts of Interest: None.
- We hereby confirm that all the Figures and Tables in the manuscript are mine ours. Besides, the Figures and images, which are not mine ours, have been given the permission for re-publication attached with the manuscript.
- Ethical Clearance: The project was approved by the local ethical committee in University of Baghdad.

References:

1. David A. Predicting the performance of organic corrosion inhibitors. *Metals*. 2017;7(553):1-8.
2. El-Bakri Y, Boudalia M, Echihi S, Harmaoui A, Sebhaoui J, Elmsellem H, et al. Performance and theoretical study on corrosion inhibition of new triazolopyrimidine derivative for carbon steel in hydrochloric acid. *J. Mat. Envir. Sci*. 2017;8(2):378-388.
3. Yadav M, Kumar S, Behera D, Bahadur I, Ramjugernath D. Electrochemical and quantum chemical studies on adsorption and corrosion inhibition performance of quinoline-thiazole derivatives on mild steel in hydrochloric acid solution. *Int. J. Electrochem. Sci*. 2014;9:5235–5257.
4. Louadi YE, Abrigach F, Bouyanzer A, Touzani R, El Assry A, Zarrouk A, et al. Theoretical and experimental studies on the corrosion inhibition potentials of two tetrakispyrazole derivatives for mild steel in 1.0M HCl. *Port. Electrochim. Acta*. 2017;35(3):159-178.
5. Kitagawa W, Tamura TA. Quinoline antibiotic from rhodococcus erythropolis JCM 6824. *J. Antibiot*. 2008;61(11): 680–682.
6. Kubba RM, Challob DA, Hussen SM. Quantum mechanical and electrochemical study of new isatin derivative as corrosion inhibitor for carbon steel in 3.5 % NaCl. *Int. J. Sci. Res*. 2017; 6 (7);1656-1669.
7. GneDy PO, Palmer R, RoocEne H, Svrn P. Isolation of aeromonassalmonicida strains resistant to the quinoline antibiotics. *Bull. Eur. Ass. Fish parhol*. 1987;7(2):43.
8. Fu H-G, Li Z.-W, Hu X.-X, Si S-Y, You X.-F, Tang S, et al. Synthesis and biological evaluation of quinoline derivatives as a novel class of broad-spectrum antibacterial agents. *Molecules* . 2019; 24 :548.
9. Singh P, Srivastava V, Quraishi MA. Novel quinoline derivatives as green corrosion inhibitors for mild steel in acidic medium: electrochemical, SEM, AFM, and XPS studies. *J. Mol. Liq*. 2016;216:164–173.

10. Elyoussfi A, Dafali A, Elmsellem H, Bouzian Y, bouhfid R, Zarrouk A, et al. Some quinoline derivatives: Synthesis and comparative study towards corrosion of mild steel in 0.5M H₂SO₄. Der Pharma Chemica. 2016;8(4):226-236.
11. Naik UJ, Jha PC, Lone MY, Shah RR, Shah NK. Electrochemical and theoretical investigation of the inhibitory effect of two Schiff bases of benzaldehyde for the corrosion of aluminium in hydrochloric acid. J. Mol. Str. 2016;1125:63–72.
12. Saha SK, Ghosh P, Hens A, Murmu NC, Banerjee P. Density functional theory and molecular dynamics simulation study on corrosion inhibition performance of mild steel by mercapto-quinoline Schiff base corrosion inhibitor. Physica E. 2015;66:332–341.
13. Sundaram RG, Sundaravadevelu M. Electrochemical and surface Investigation of quinoline-8-sulphonyl chloride as corrosion inhibitor for mild steel in acidic medium. Int J Chem Tech Res. 2016;9:527–539.
14. Al-Bayati RI, Ahamad MR, Ahamed LS. Synthesis and biological activity investigation of some quinoline-2-one derivatives. Amer. J. Org. Chem. 2015;5(4):125-135
15. Kubba RM, Al-Majidi SMH, Ahmed A.H. Synthesis, characterization and quantum chemical studies of inhibition ability of novel 5-nitro isatin derivatives on the corrosion of carbon steel in sea water. Iraq. J. Sci. 2019;60(4):688-705.
16. Frisch MJ, Pople JA. Gaussian 09, Revision E.01. Gaussian, Inc., Wallingford CT. 2009.
17. Becke, A Density-functional thermochemistry. III. The role of exact exchange. J. Chem. Phys.1993; 98:5648-5652.
18. Kubba RM, Al-Majidi SMH, Ahmed AH. Synthesis, identification, theoretical and experimental studies for carbon steel corrosion inhibition in seawater for new urea and thiourea derivatives linkage to 5-nitro isatin moiety . Der Pharma. Chemica. 2018;10(7):86-99.
19. Parr RG, Yang W. Density Functional Theory of Atoms and Molecules. 1ST Ed., 1989,Oxford University Press: New York.
20. Kubba RM, Alag AS. Experimental and theoretical evaluation of new quinazolinone derivative as organic corrosion inhibitor for carbon steel in 1M HCl solution. IJSR. 2017;6(6):1832-1843.
21. Duboscq J, Sabot R, Jeannin M, Refait P. Localized corrosion of carbon steel in seawater: processes occurring in cathodic zones. Mat. Corr. 2019;70(6): 973-984.
22. Fleming I. Frontier Orbitals and Organic Chemical Reactions. John Wiley and Sons, NewYork, 1976.
23. Chermette, H. Chemical reactivity indexes in density functional theory. J. Comp. Chem. 1999;20:129-154.
24. Pearson RG. Absolute electronegativity and hardness application to inorganic chemistry. Inorg. Chem. 1988;27(4): 734–740.
25. Kubba RM, Mohammed M. Synthesis, Identification, Theoretical and experimental studies of carbon steel corrosion inhibition in seawater by some new diazine derivatives linked to 5-nitroisatin moiety. Iraq. J. Sci. 2018;59(3B):1347-1365.
26. Singh A, Ansari KR, Lin Y, Quraishi, MA, Lgaz H, Chung. III-M. Corrosion inhibition performance of imidazolidine derivatives for J55 pipeline steel in acidic oilfield formation water: Electrochemical, surface and theoretical studies. J. Taiw. Inst. Chem. Eng. 2019;95:341-356.
27. Ahmed AH, Al-Majidi SMH, Kubba RM. Surface protection of carbon steel by butane sulphonic acid-zinc ion system. J. Glob. Pharma. Tech. 2018;10(05):369-383.
28. Liu Y, Wang Z, Wei Y. Influence of seawater on the carbon steel initial corrosion behavior. Int. J. Electrochem. Sci. 2019;14:1147–1162.

حسابات DFT ودراسة تجريبية لتثبيط تآكل حديد الصلب الكربوني في محلول ملحي بفعل مشتق للكينولين-2-اون

لمى سامي أحمد

مصطفى علاء محمد

رحاب ماجد كبة

قسم الكيمياء، كلية العلوم، جامعة بغداد، بغداد، العراق

الخلاصة:

تم إجراء دراسة نظرية وتجريبية على حماية تآكل سطح حديد الصلب الكربوني عند تراكيز مختلفة من المشتق (الكينولين-2-اون) الذي يحمل الاسم: *1-Amino-4,7-dimethyl-6-nitro-1H-quinolin-2-one* (ADNQ2O). من الناحية النظرية، تم استخدام نظرية دالة الكثافة (DFT) عند المستوى 6-311++G (2d,2p) (B3LYP) لحساب التركيب الهندسي والخصائص الفيزيائية ومعايير كفاءة التثبيط الكيميائية، مع مواقع الامتزاز الفعالة من أجل التنبؤ بمعرفة المواقع المحتملة للهجمات النكليوفيلية والالكتروفيلية، في الفراغ و في اثنين من المذيبات (DMSO) و (H₂O)، كل ذلك عند الأشكال الهندسية التوازنية. من الناحية التجريبية، تمت دراسة كفاءة التثبيط (%IE) في محلولي NaCl (3.5%) باستخدام قياسات الاستقطاب الجهادي. أظهرت النتائج أن كفاءة التثبيط (%IE) في المحلول الملحي (% 89.88). و تدعم معلمات الديناميكية الحرارية التي تم الحصول عليها آلية الامتزاز الفيزيائي. وأن الامتزاز على سطح حديد الصلب الكربوني يطبع ايزوثيرم امتزاز لنكماير isotherm Langmuir. وتمت دراسة التغيرات السطحية لحديد الصلب الكربوني باستخدام تقنية الفحص المجهرية للإلكترون (SEM).

الكلمات المفتاحية: سلوك التآكل، DFT ، الكينولين، معلمات الديناميكية الحرارية.